Neural Comput & Applic (2019) 31:199–205
DOI 10.1007/s00521-017-3013-9

ORIGINAL ARTICLE

On stratified variable thermal conductivity stretched flow of Walter-B material subject to non-Fourier flux theory

T. Hayat[1,2] · M. Zubair[1] · M. Waqas[1] · A. Alsaedi[2] · M. Ayub[1]

Received: 30 November 2016 / Accepted: 11 April 2017 / Published online: 3 May 2017

Abstract The objective here is to examine the characteristics of non-Fourier flux theory in flow induced by a nonlinear stretched surface. Constitutive expression for an incompressible Walter-B liquid is taken into account. Consideration of thermal stratification and variable thermal conductivity characterizes the heat transfer process. The concept of boundary layer is adopted for the formulation purpose. Modern methodology for the computational process is implemented. Surface drag force is computed and discussed. Salient features of significant variables on the physical quantities are reported graphically. It is explored that velocity is enhanced for a larger ratio of rate constants. The increasing values of thermal relaxation factor correspond to less temperature.

Keywords Thermal stratification · Walter-B material · Non-Fourier flux theory · Stagnation point flow · Variable thermal conductivity

1 Introduction

An impressive consideration has been given to heat conduction [1–3] because of its ample applications in several fields. The traditional one-dimensional (1D) fundamental model to characterize heat conduction is analyzed through Fourier's relation [4]. This yields an approach to analyze heat conduction and develops the foundation to investigate the thermal process of heat transfer in recent years. However, an ambiguity of Fourier's model [5–7] is that the whole structure is affected directly by the original disruption. Such behavior disprove the causality principle [8, 9] through heat conduction paradox. Cattaneo [10] recommended a generalized model which yields the relaxation factor into account. The Cattaneo basic expression only comprises partial time derivatives whereas larger spatial gradients might be needed [11] for the entire process. Hence, modifying the "time derivative" by "Oldroyds' upper-convected derivative," Christov [12] recommended the frame-indifferent modification of the Cattaneo expression:

$$\mathbf{q}+\lambda\left(\frac{\partial \mathbf{q}}{\partial t}+\mathbf{v}.\nabla\mathbf{q}-\mathbf{q}.\nabla\mathbf{v}+(\nabla.\mathbf{v})\mathbf{q}\right)=-k\,\mathrm{grad}T.$$

Here ($\mathbf{q}$, λ, $\mathbf{v}$, k, T) indicate heat flux, thermal relaxation parameter, velocity, thermal conductivity, and temperature, respectively. The aforementioned expression justifies objectivity principle and fascinates the attention of recent investigators [13–25].

Fluid flow and heat transport characteristics over a flat or stretched surface have turned to be the ground of great importance due to their numerous applications in plastic and rubber sheet manufacturing, filaments and polymer sheets, glass blowing, etc. Stretching flow towards a flat surface is firstly explored by Crane [26]. Moreover, plates in usage with variable thickness are utilized in marine and aeronautical configurations and mechanical and civil engineering. For reliable and effective design, it is essential to consider buckling loads for these plates. No doubt the usage of variable thickness supports to decrease the load of mechanical elements and develop the effectiveness of

✉ M. Waqas
mwaqas@math.qau.edu.pk

1 Department of Mathematics, Quaid-I-Azam University, 45320, Islamabad 44000, Pakistan

2 Nonlinear Analysis and Applied Mathematics (NAAM) Research Group, Department of Mathematics, Faculty of Science, King Abdulaziz University, P. O. Box 80257, Jeddah 21589, Saudi Arabia

materials [27]. Few studies comprising the simultaneous characteristics of variable thickness and heat transfer can be found in the attempts [28–32].

Although required in definite utilizations, thermal stratification influences the performance of the condenser and could be destructive for structural reliability of the pool walls prepared through concrete. Analysis on rigidly stratified medium demonstrates that stationary regions are energetic at the boundary of cold and hot water, which minimizes the service lifetime of plants and several demanding components [33]. For instance, the blight heat elimination process in fast devices encounters the phenomenon of stratification at relatively high temperature producing exhaustion in nuclear mechanisms. Thus, from the structural security opinion as well, stratified coolant aspects are significant [34]. Representative studies on thermal stratification are given in [35–37]. Moreover, the ability of a substance to control heat is recognized as thermal conductivity. It is either constant or differs with temperature linearly for liquid metals from 0 to 400 °F [38]. Representative investigations regarding this topic can be mentioned through [39–42] and several studies therein.

The current investigation intends to analyze the non-Fourier flux characteristics in flow of Walter-B material over the surface with variable thickness. Stagnation velocity is considered nonlinear. Heat transfer in the presence of thermal stratification and temperature-dependent thermal conductivity is analyzed. A homotopic algorithm [43–50] is utilized to obtain convergent expressions. Graphical trends for several significant variables versus velocity and temperature fields are discussed in detail.

2 Formulation

Here steady two-dimensional stagnation point flow of Walter-B material towards a surface moving with nonlinear velocity is modeled. A stretching surface of variable thickness generates the flow. Heat transfer via non-Fourier flux theory is investigated. Thermal stratification along with temperature-dependent thermal conductivity is retained. Viscous dissipation effects are not accounted. The governing equations are

$$\frac{\partial u}{\partial x}+\frac{\partial v}{\partial y}=0, \tag{1}$$

$$u\frac{\partial u}{\partial x}+v\frac{\partial u}{\partial y}=U_e\frac{dU_e}{dx}+\frac{\mu_0}{\rho}\left(\frac{\partial^2 u}{\partial y^2}\right)-\frac{k_0}{\rho}\left(\begin{array}{c} u\frac{\partial^3 u}{\partial x\partial y^2}+v\frac{\partial^3 u}{\partial y^3} \\ -\frac{\partial u}{\partial y}\frac{\partial^2 u}{\partial x\partial y}+\frac{\partial v}{\partial y}\frac{\partial^2 u}{\partial y^2}\end{array}\right), \tag{2}$$

$$u\frac{\partial T}{\partial x}+v\frac{\partial T}{\partial y}+\lambda\left(\begin{array}{c} u\frac{\partial u}{\partial x}\frac{\partial T}{\partial x}+v\frac{\partial v}{\partial y}\frac{\partial T}{\partial y}+u\frac{\partial v}{\partial x}\frac{\partial T}{\partial y}+v\frac{\partial u}{\partial y}\frac{\partial T}{\partial x} \\ +2uv\frac{\partial^2 T}{\partial x\partial y}+u^2\frac{\partial^2 T}{\partial x^2}+v^2\frac{\partial^2 T}{\partial y^2}\end{array}\right) =\frac{1}{\rho c_p}\frac{\partial}{\partial y}\left(k(T)\frac{\partial T}{\partial y}\right), \tag{3}$$

$$u=U_w(x)=U_0(x+b)^n, v=0, T=T_w = T_0+c(x+b) \text{ at } y=A_1(x+b)^{\frac{1-n}{2}}, \tag{4}$$

$$u\to U_e(x)=U_\infty(x+b)^n, T\to T_\infty=T_0+d(x+b) \text{ when } y\to\infty. \tag{5}$$

Here (u, v) specify the liquid velocities parallel to horizontal and vertical directions, $\nu=\left(\frac{\mu}{\rho}\right)$ the kinematic viscosity, ρ the fluid density, (k_0, μ_0) the short memory coefficient and restricting viscosity at low shear rate, $(U_w(x), U_e(x))$ the stretching and free stream velocities, (T, T_∞) the fluid and ambient fluid temperature, (U_0) the reference velocity, (b, c, d) the dimensional constants, A_1 the small variable with respect to the surface is adequately thin, and $k(T)$ the temperature-dependent thermal conductivity, which is given as [20]

$$k(T)=k_\infty\left(1+\varepsilon\frac{T-T_\infty}{\nabla T}\right). \tag{6}$$

Here, ambient fluid thermal conductivity is denoted by k_∞, ε is the small parameter which characterizes the behavior of temperature on thermal conductivity and $\nabla T = T - T_0$. Also, the type of motion, surface shape and characteristics of the boundary layer can be controlled through the parameter n. It is worth pointing that the present analysis reduced to a surface with growing thickness and convex outer shape, whereas the analysis converted to a surface with growing thickness and convex outer shape when $n < 1$. Also, for $n = 0$, the motion is reduced to a linear case with constant velocity. Considering [16],

$$\psi=\sqrt{\frac{2}{n+1}\nu U_0(x+b)^{n+1}}F(\xi), \xi=\sqrt{\frac{n+1}{2}\frac{U_0}{\nu}(x+b)^{n-1}}y, u=U_0(x+b)^n F'(\xi),$$
$$v=-\sqrt{\frac{n+1}{2}\nu U_0(x+b)^{n-1}}\left(F(\xi)+\eta\frac{n-1}{n+1}F'(\xi)\right), \Theta(\xi)=\frac{T-T_\infty}{T_w-T_0}, \tag{7}$$

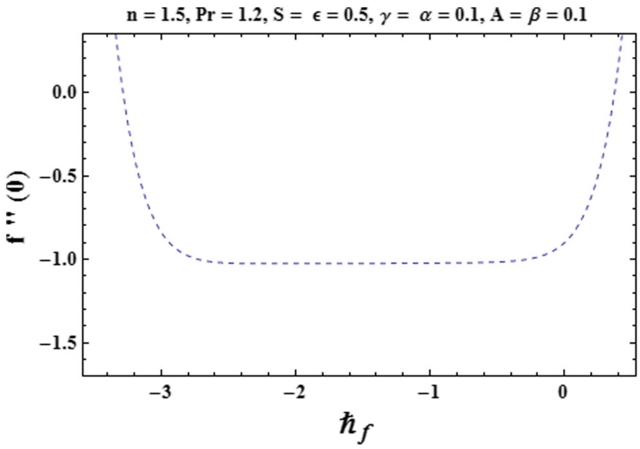

Fig. 1 $\hbar$-curve for f

the continuity equation ((1)) is fulfilled automatically and the emerging nonlinear problems in F and Θ are

$$F'''-\frac{2n}{n+1}F'^2+FF''+\beta\left(\frac{3n-1}{2}F''^2-(3n-1)F'F'''+\frac{n+1}{2}FF^{iv}\right)+\frac{2n}{n+1}A^2=0, \tag{8}$$

$$(1+\varepsilon\Theta)\Theta''+\varepsilon\Theta'^2+\Pr F\Theta'+\Pr\gamma\begin{pmatrix}\frac{n-3}{2}FF'\Theta'\\-\frac{n+1}{2}F^2\Theta''\end{pmatrix}+\Pr(S+\Theta)\begin{pmatrix}\gamma FF''\\-\frac{2n}{n+1}\gamma F'^2-\frac{2}{n+1}F'\end{pmatrix}=0, \tag{9}$$

$$F(\alpha)=\alpha\frac{1-n}{1+n},\ F'(\alpha)=1,\ F'(\infty)=A, \tag{10}$$

$$\Theta(\alpha)=1-S,\ \Theta(\infty)=0. \tag{11}$$

Here, prime signifies differentiation with respect to ξ and $\alpha=A_1\sqrt{\frac{n+1}{2}\frac{U_0}{\nu}}$. Letting $F(\xi)=f(\xi-\alpha)=f(\eta)$ and $\Theta(\xi)=\theta(\xi-\alpha)=\theta(\eta)$, Eqs. (8)–(11) yield

$$f'''-\frac{2n}{n+1}f'^2+ff''+\beta\left(\frac{3n-1}{2}f''^2-(3n-1)f'f'''+\frac{n+1}{2}ff^{iv}\right)+\frac{2n}{n+1}A^2=0, \tag{12}$$

$$(1+\varepsilon\theta)\theta''+\varepsilon\theta'^2+\Pr f\theta'+\Pr\gamma\begin{pmatrix}\frac{n-3}{2}ff'\theta'\\-\frac{n+1}{2}f^2\theta''\end{pmatrix}+\Pr(S+\theta)\begin{pmatrix}\gamma ff''\\-\frac{2n}{n+1}\gamma f'^2-\frac{2}{n+1}f'\end{pmatrix}=0, \tag{13}$$

$$f(0)=\alpha\frac{1-n}{1+n},\quad f'(0)=1,\ f'(\infty)=A, \tag{14}$$

$$\theta(0)=1-S,\ \theta(\infty)=0, \tag{15}$$

where $A\left(=\frac{U_\infty}{U_0}\right)$ represents the ratio of velocities, $\Pr\left(=\frac{\mu c_p}{k}\right)$ the Prandtl number, $\beta\left(=\frac{k_0U_0(x+b)^{n-1}}{\mu_0}\right)$ the local

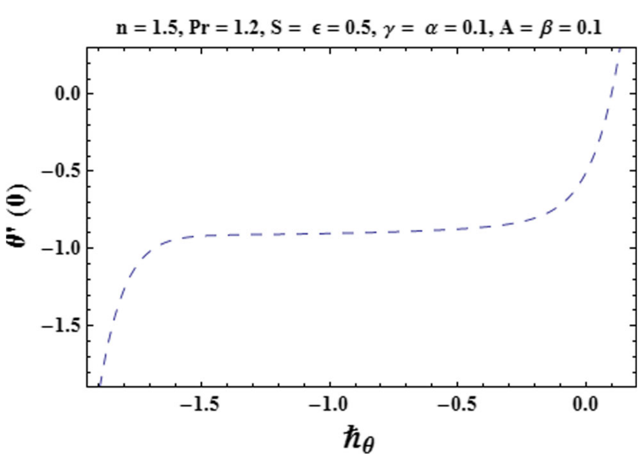

Fig. 2 $\hbar$-curve for θ

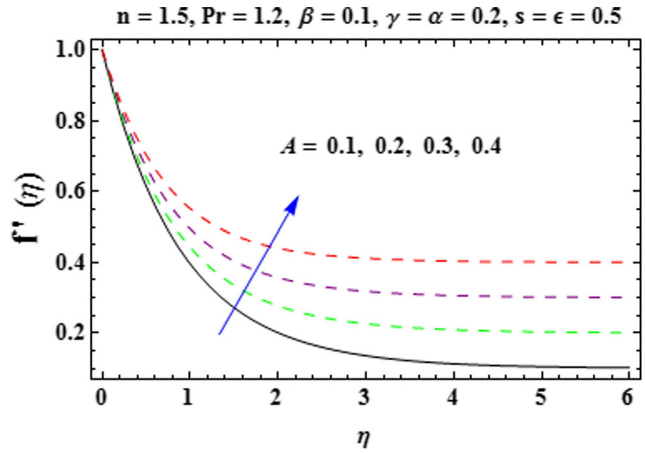

Fig. 3 A variation on f'

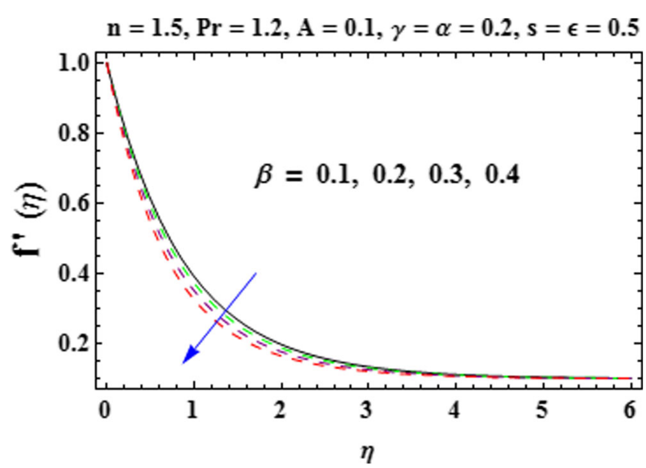

Fig. 4 β variation on f'

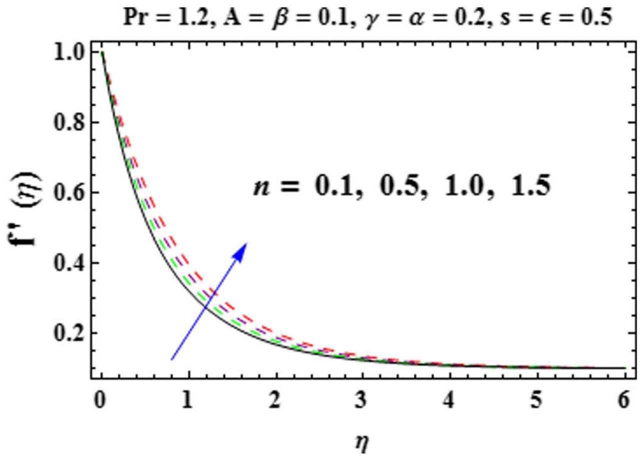

Fig. 5 n variation on f'

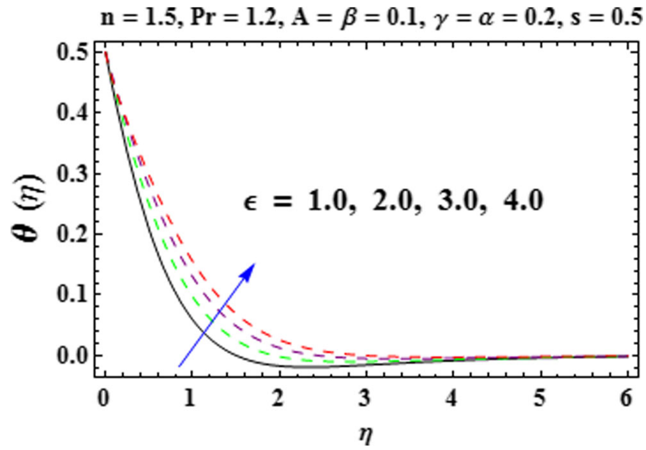

Fig. 7 ε variation on θ

Weissenberg number, $S\left(=\frac{d}{c}\right)$ the thermal stratification parameter, and $\gamma(=\lambda U_0(x+b)^{n-1})$ the relaxation factor.

Our analysis reduces to Fourier's situation when $\gamma=0$ in Eq. (13).

The skin friction coefficient is defined as

$$C_f = \frac{\tau_w}{\frac{1}{2}\rho u_w^2}, \tag{16}$$

with

$$\tau_w = \mu_0\left(\frac{\partial u}{\partial y}\right)_{y=A_1(x+b)^{\frac{1-n}{2}}} - k_0\left(u\frac{\partial^2 u}{\partial x\partial y} - 2\frac{\partial u}{\partial x}\frac{\partial u}{\partial y}\right)_{y=A_1(x+b)^{\frac{1-n}{2}}}. \tag{17}$$

Utilizing Eq. (17) in Eq. (16), the dimensionless form of the skin friction coefficient is given below:

$$\sqrt{\mathrm{Re}_x}C_f = \sqrt{\frac{n+1}{2}}\left(\left[1-\beta\left(\frac{7n-1}{2}f'-2\eta\frac{n-1}{2}f''\right)\right]f'' + \beta\eta\frac{n-1}{2}f'f'''\right)_{\eta=0}, \tag{18}$$

with $\mathrm{Re}_x = u_w(x)(x+b)/\nu$ showing the local Reynolds number.

3 Series solutions via homotopic procedure

Our intention here is to compute the convergent solution expressions for Eqs. (12) and (13) along with conditions (14) and (15). For this purpose, the initial approximations and linear operators are considered as

$$f_0(\eta) = A\eta + (1-A)\left(1-e^{-\eta}\right) + \alpha\frac{1-n}{1+n}, \theta_0(\eta) = (1-S)e^{-\eta}, \tag{19}$$

$$L_f = f''' - f', L_\theta = \theta'' - \theta, \tag{20}$$

with

$$L_f\left(C_1 + C_2e^{\eta} + C_3e^{-\eta}\right) = 0, L_\theta\left(C_4e^{\eta} + C_5e^{-\eta}\right) = 0, \tag{21}$$

in which $C_i(i=1-5)$ signify the arbitrary constants.

Convergence of secured obtained solutions is verified through the homotopy analysis method (HAM). Auxiliary variables ($\hbar_f$, $\hbar_\theta$) involved in formulated series solutions are

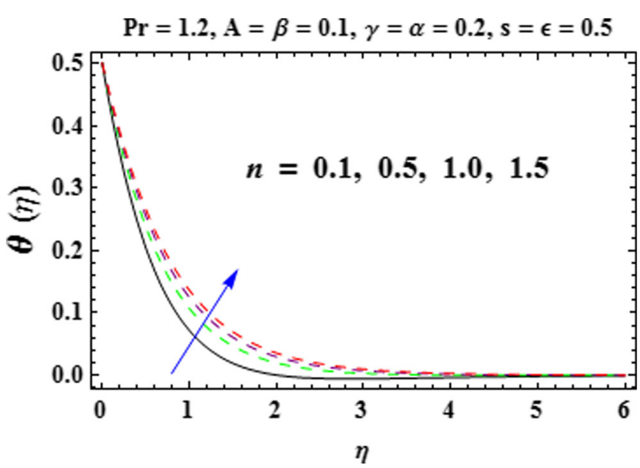

Fig. 6 n variation on θ

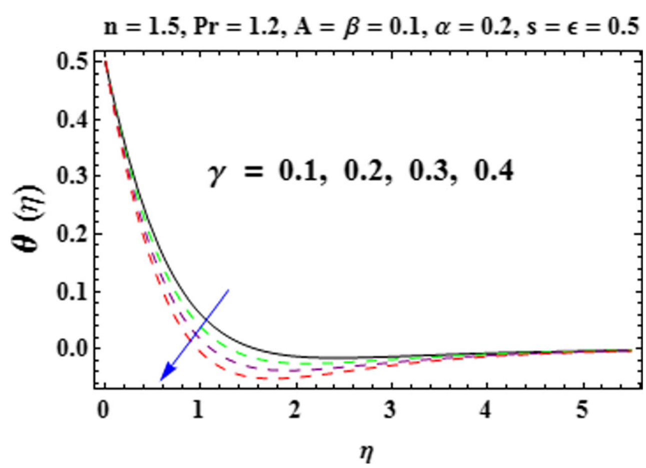

Fig. 8 γ variation on θ

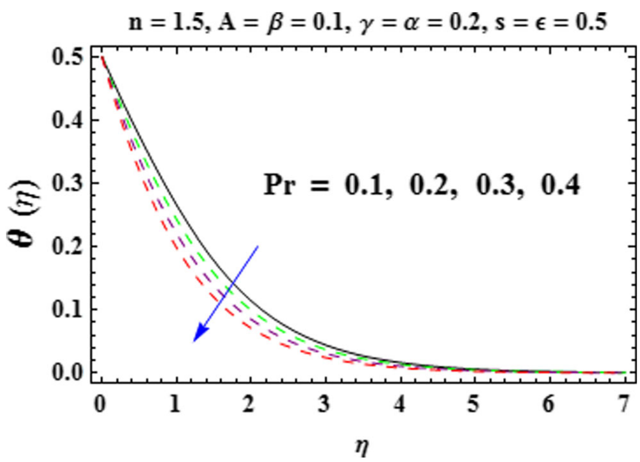

Fig. 9 Pr variation on θ

Table 1 Convergence of HAM expression for various orders of deformations when $n = 1.5$, $A = \gamma = K_2 = 0.2, K_1 = 0.1, S = 0.3$, $\alpha = \varepsilon = 0.5$, $\Pr = 1.2$, and $\hbar_f = \hbar_\theta = -0.9$

Order of approximations	$-f''(0)$	$-\theta'(0)$
1	1.0110	0.9447
5	1.0213	0.9185
10	1.0243	0.9038
15	1.0254	0.9214
20	1.0259	0.9236
25	1.0262	0.9275
30	1.0262	0.9275
35	1.0262	0.9275
40	1.0262	0.9275

significant for such motivation. Thus, Figs. 1 and 2 highlight the plots for 12th order of approximations. The values verifying the convergence are in the ranges $-1.40 \le \hbar_f \le -0.20$ and $-1.65 \le \hbar_\theta \le -0.90$.

4 Discussion

This section highlights the salient characteristics of the ratio of velocities (A), Prandtl number (Pr), local Weissenberg number (β), thermal stratification parameter (S), thermal relaxation factor (γ), and power index (n) on velocity $f'(\eta)$ and temperature $\theta(\eta)$ through Figs. 3, 4, 5, 6, 7, 8, 9, and 10.

Figure 3 communicates the behavior of A on $f'(\eta)$. It is remarked that $f'(\eta)$ boosts via larger A. Impact of β on $f'(\eta)$ is reported through Fig. 4. Larger β reduces $f'(\eta)$, which relates to a thinner momentum layer. Physically, viscoelasticity yields tensile stress which diminishes the boundary layer and thus $f'(\eta)$ reduces. Figure 5 characterizes the features of n on $f'(\eta)$. Clearly $f'(\eta)$ shows increasing behavior for larger n. Actually, stretching velocity rises for larger n and consequently more deformation in the fluid is generated. Thus, $f'(\eta)$ rises.

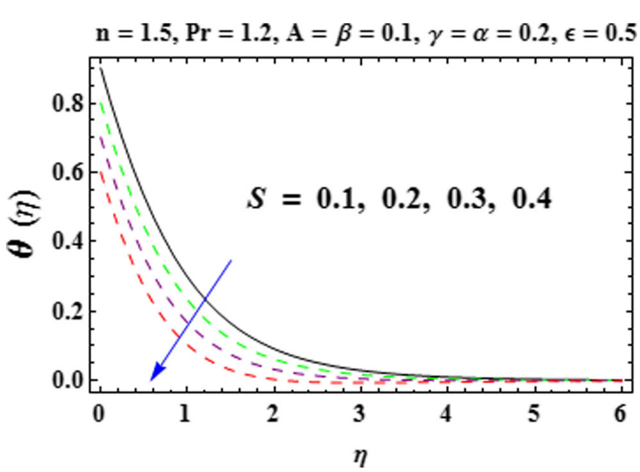

Fig. 10 S variation on θ

Characteristics of n on $\theta(\eta)$ are disclosed through Fig. 6. It is explored that both $\theta(\eta)$ and thermal layer thickness boost for larger n. Effect of ε on $\theta(\eta)$ is portrayed via Fig. 7. Here, $\theta(\eta)$ augments when ε is increased. In fact, thermal conductivity rises through larger ε, due to which a considerable amount of heat moves from the sheet to the material. Therefore, $\theta(\eta)$ augments. Figure 8 highlights the influence of γ on $\theta(\eta)$. Here, $\theta(\eta)$ decays for higher γ. From the physical point of view, elements of the material need more time to transport heat to its adjacent elements, due to which $\theta(\eta)$ decays. Salient features of S on $\theta(\eta)$ is depicted in Fig. 9. It is noticed that $\theta(\eta)$ and the associated layer thickness decay for higher S. Physically, temperature difference reduces between the surface of the sheet and liquid, which generates the reduction in $\theta(\eta)$. Figure 10 explores the impact of Pr on $\theta(\eta)$. As expected, $\theta(\eta)$ and the corresponding layer thickness reduce when Pr is enhanced. An enhancement in Pr corresponds to a slow rate of thermal diffusion.

Convergence of series solution is verified numerically through Table 1. It is noticed that the 25th order of deformations are acceptable regarding convergent expressions of velocity and temperature. Characteristics of β and A on surface drag force $\left(C_f \mathrm{Re}_x^{1/2}\right)$ is disclosed through Table 2. Here, $C_f \mathrm{Re}_x^{1/2}$ decays via larger β and A. Table 3 delivers the comparative analysis of skin friction coefficient (i.e., when $\beta = 0$ and

Table 2 Skin friction $\left(C_f \mathrm{Re}_x^{1/2}\right)$ for distinct values of parameters β and A when $n = 1.5$, γ=0.2,S = 0.3, $\varepsilon = 0.5$,$\alpha = 0.2$, and $\Pr = 1.2$

β	A	$C_f \mathrm{Re}_x^{1/2}$
0.0	0.1	−0.9668
0.2		−0.4372
0.4		−0.2561
0.1	0.0	−0.7376
	0.2	−0.6843
	0.4	−0.5806

Table 3 Comparative analysis of obtained results of $f''(0)$ with [51] when $n = 1$ and $\beta = 0$

A	Ref. [51]	Present
0.1	−0.9694	−0.96939
0.2	−0.9181	−0.91811
0.5	−0.6673	−0.66726
0.7		−0.43346
0.8		−0.29929
0.9		−0.15458
1.0		0.00000

$n = 1$) with the work of Mahapatra and Gupta [51]. Reasonable agreement is observed.

5 Final remarks

Here non-Fourier heat flux in stagnation point flow towards nonlinear stretching flow of Walter's B material is addressed. The main findings are summarized below.

- There is reverse behavior of A and β on $f'(\eta)$ qualitatively.
- Temperature ($\theta(\eta)$) via γ and Pr is less when compared with ε.
- Fourier's expression has high temperature in comparison to non-Fourier expression.
- Surface drag force decays for larger A and β.
- Viscous material results can be achieved by putting $\beta = 0$.

Compliance with ethical standards

Conflict of interest The authors declare that they have no conflict of interest.

References

1. Ozisik MN (1993) Heat conduction (third ed.). John Wiley & Sons, New York
2. Garrido PL, Hurtado PI, Nadrowski B (2001) Simple one-dimensional model of heat conduction which obeys Fourier's law. Phys Rev Lett 86:5486–5489
3. Kabir MM (2011) Analytic solutions for generalized forms of the nonlinear heat conduction equation. Nonlinear Anal RWA 12: 2681–2691
4. Guo SL, Wang BL (2015) Thermal shock fracture of a cylinder with a penny-shaped crack based on hyperbolic heat conduction. Int J Heat Mass Transf 91:235–245
5. Christov CI, Jordan PM (2005) Heat conduction paradox involving second-sound propagation in moving media. Phys Rev Lett 94: 154301
6. Qi HT, Guo XW (2014) Transient fractional heat conduction with generalized Cattaneo model. Int J Heat Mass Transf 76:535–539
7. Ying XH, Tao QH, Yun JX (2013) Fractional Cattaneo heat equation in a semi-infinite medium. Chin Phys B 22:014401
8. Zhao X, Sun ZZ (2015) Compact Crank-Nicolson schemes for a class of fractional Cattaneo equation in inhomogeneous medium. J Sci Comput 62:747–771
9. Qi HT, Jiang XY (2011) Solutions of the space-time fractional Cattaneo diffusion equation. Phys A 390:1876–1883
10. Cattaneo C (1948) Sulla conduzione del calore, Atti semin. Mat. Fis. Univ. Modena Reggio Emilia 3:83–101
11. Liu L, Zheng L, Zhang X (2016) Fractional anomalous diffusion with Cattaneo–Christov flux effects in a comb-like structure. Appl Math Model 40:6663–6675
12. Christov CI (2009) On frame indifferent formulation of the Maxwell-Cattaneo model of finite-speed heat conduction. Mech Res Commun 36:481–486
13. Nadeem S, Muhammad N (2016) Impact of stratification and Cattaneo-Christov heat flux in the flow saturated with porous medium. J Mol Liq 224:423–430
14. Waqas M, Hayat T, Farooq M, Shehzad SA, Alsaedi A (2016) Cattaneo-Christov heat flux model for flow of variable thermal conductivity generalized Burgers fluid. J Mol Liq 220:642–648
15. Khan WA, Khan M, Alshomrani AS (2016) Impact of chemical processes on 3D Burgers fluid utilizing Cattaneo-Christov double-diffusion: applications of non-Fourier's heat and non-Fick's mass flux models. J Mol Liq 223:1039–1047
16. Hayat T, Zubair M, Ayub M, Waqas M, Alsaedi A (2016) Stagnation point flow towards nonlinear stretching surface with Cattaneo-Christov heat flux. Eur Phys J Plus 131:355
17. Liu L, Zheng L, Liu F, Zhang X (2016) Anomalous convection diffusion and wave coupling transport of cells on comb frame with fractional Cattaneo-Christov. Comm Non Sci Numer Simul 38:45–58
18. Hayat T, Khan MI, Farooq M, Alsaedi A, Waqas M, Yasmeen T (2016) Impact of Cattaneo-Christov heat flux model in flow of variable thermal conductivity fluid over a variable thicked surface. Int J Heat Mass Transf 99:702–710
19. Tanveer A, Hina S, Hayat T, Mustafa M, Ahmad B (2016) Effects of the Cattaneo-Christov heat flux model on peristalsis. Eng Applications Comput Fluid Mech 10:375–385
20. Hayat T, Waqas M, Shehzad SA, Alsaedi A (2016) On 2D stratified flow of an Oldroyd-B fluid with chemical reaction: an application of non-Fourier heat flux theory. J Mol Liq 223:566–571
21. Sui J, Zheng L, Zhang X (2016) Boundary layer heat and mass transfer with Cattaneo-Christov double-diffusion in upper-convected Maxwell nanofluid past a stretching sheet with slip velocity. Int J Thermal Sci 104:461–468
22. Khan WA, Khan M, Alshomrani AS, Ahmad L (2016) Numerical investigation of generalized Fourier's and Fick's laws for Sisko fluid flow. J Mol Liq 224:1016–1021
23. Ali ME, Sandeep N (2017) Cattaneo-Christov model for radiative heat transfer of magnetohydrodynamic Casson-ferrofluid: a numerical study. Results Phys 7:21–30
24. Hayat T, Khan MI, Waqas M, Alsaedi A (2017) On Cattaneo–Christov heat flux in the flow of variable thermal conductivity Eyring–Powell fluid. Results Phys DOI. doi:10.1016/j.rinp.2016.12.034
25. Kumar KA, Reddy JVR, Sugunamma V, Sandeep N (2016) Magnetohydrodynamic Cattaneo-Christov flow past a cone and a wedge with variable heat source/sink. Alex Eng J DOI. doi:10.1016/j.aej.2016.11.013
26. Crane LJ (1970) Flow past a stretching plate. J Appl Math Phys (ZAMP) 21:645–647
27. Shufrin I, Eisenberger M (2005) Stability of variable thickness shear deformable plates-first order and high order analyses. Thin-Walled Struct 43:189–207
28. Subhashini SV, Sumathi R, Pop I (2013) Dual solutions in a thermal diffusive flow over a stretching sheet with variable thickness. Int Commun Heat Mass Transfer 48:61–66

29. Hayat T, Hussain Z, Muhammad T, Alsaedi A (2016) Effects of homogeneous and heterogeneous reactions in flow of nanofluids over a nonlinear stretching surface with variable surface thickness. J Mol Liq 221:1121–1127
30. Hayat T, Bashir G, Waqas M, Alsaedi A (2016) MHD 2D flow of Williamson nanofluid over a nonlinear variable thicked surface with melting heat transfer. J Mol Liq 223:836–844
31. Hayat T, Khan MI, Waqas M, Alsaedi A (2017) Mathematical modeling of non-Newtonian fluid with chemical aspects: a new formulation and results by numerical technique. Colloids Surfaces A: Physicochemical Eng Aspects DOI. doi:10.1016/j.colsurfa.2017.01.007
32. Hayat T, Zubair M, Ayub M, Waqas M, Alsaedi A (2017) On doubly stratified chemically reactive flow of Powell-Eyring liquid subject to non-Fourier heat flux theory. Results Phys 7:99–106
33. Opanasenko AN, Sorokin AP, Zaryugin DG, Rachkov MV (2012) Coolant stratification in nuclear power facilities. Atomic Energy 111:172–178
34. Parthasarathy U, Sundararajan T, Balaji C, Velusamy K, Chellapandi P, Chetal SC (2012) Decay heat removal in pool type fast reactor using passive systems. Nuc Eng Des 250:480–499
35. Lu T, Han WW, Zhai H (2015) Numerical simulation of temperature fluctuation reduction by a vortex breaker in an elbow pipe with thermal stratification. Annals Nuc Energy 75:462–467
36. Kumar S, Vijayan PK, Kannan U, Sharma M, Pilkhwal DS (2017) Experimental and computational simulation of thermal stratification in large pools with immersed condenser. Appl Thermal Eng 113:345–361
37. Hayat T, Khan MI, Farooq M, Alsaedi A, Khan MI (2017) Thermally stratified stretching flow with Cattaneo-Christov heat flux. Int J Heat Mass Transf 106:289–294
38. Chiam CT (1966) Heat transfer with variable conductivity in stagnation-point flow towards a stretching sheet. Int Commun Heat Mass Transfer 23:239–248
39. Akbar NS, Raza M, Ellahi R (2016) Endoscopic effects with entropy generation analysis in peristalsis for the thermal conductivity of H_2O+Cu nanofluid. J Appl Fluid Mech 9:1721–1730
40. Akbar NS, Raza M, Ellahi R (2015) Peristaltic flow with thermal conductivity of H_2O+Cu nanofluid and entropy generation. Results Phys 5:115–124
41. Akbar NS, Raza M, Ellahi R (2016) Anti-bacterial applications for new thermal conductivity model in arteries with CNT suspended nanofluid. Int J Mech Medicine Biology 16:1650063
42. Hayat T, Khan MI, Waqas M, Yasmeen T, Alsaedi A (2016) Viscous dissipation effect in flow of magnetonanofluid with variable properties. J Mol Liq 222:47–54
43. Liao SJ (2012) Homotopic analysis method in nonlinear differential equations. Springer, Heidelberg
44. Ellahi R, Hassan M, Zeeshan A (2016) Aggregation effects on water base Al2O3-nanofluid over permeable wedge in mixed convection. Asia-Pacific J Chemical Eng 11:179–186
45. Hayat T, Waqas M, Shehzad SA, Alsaedi A (2016) A model of solar radiation and Joule heating in magnetohydrodynamic (MHD) convective flow of thixotropic nanofluid. J Mol Liq 215:704–710
46. Turkyilmazoglu M (2016) An effective approach for evaluation of the optimal convergence control parameter in the homotopy analysis method. Filomat 30:1633–1650
47. Hayat T, Waqas M, Khan MI, Alsaedi A (2016) Analysis of thixotropic nanomaterial in a doubly stratified medium considering magnetic field effects. Int J Heat Mass Transf 102:1123–1129
48. Shehzad SA, Hayat T, Alsaedi A, Chen B (2016) A useful model for solar radiation. Energy, Ecology Environment 1:30–38
49. Waqas M, Farooq M, Khan MI, Alsaedi A, Hayat T, Yasmeen T (2016) Magnetohydrodynamic (MHD) mixed convection flow of micropolar liquid due to nonlinear stretched sheet with convective condition. Int J Heat Mass Transf 102:766–772
50. Hayat T, Qayyum S, Waqas M, Alsaedi A (2016) Thermally radiative stagnation point flow of Maxwell nanofluid due to unsteady convectively heated stretched surface. J Mol Liq 224:801–810
51. Mahapatra TR, Gupta AS (2002) Heat transfer in stagnation-point flow towards a stretching sheet. Heat Mass Transf 38:517–521